

ANCHOR MOORING LINE ANALYSIS IN COHESIVE SEAFLOOR

Sangchul Bang
Professor, Department of Civil and Environmental Engineering
Dean, College of Earth Systems
South Dakota School of Mines and Technology
Rapid City, SD 57701
USA

ABSTRACT

An analytical solution method capable of determining the geometric configuration and developed tensile forces of mooring lines associated with fixed plate/pile or drag anchors is presented. The solution method, satisfying complete equilibrium conditions, is capable of analyzing multi-segmented mooring lines that can consist of either chains, cables, or wires embedded in layered seafloor soils. Centrifuge model tests and full -scale field tests were used to calibrate and validate the analytical solution.

INTRODUCTION

The US Navy has initiated the development of an analytical solution method that can analyze offshore and deep water mooring lines associated with embedded drag and fixed anchors (1, 2). Mooring lines may be comprised of multi-segments with different material and/or geometric properties and embedded in a general seafloor soil having either cohesion or friction or both. Any number of sinkers can also be added to the suspended portion of the mooring line within the water. Solutions can be obtained with a fixed total length of the mooring line, a fixed horizontal length of the mooring line, or a fixed exit angle of the mooring line at the seafloor surface.

This paper describes the principles associated with the development of the solution for the mooring line analysis. Also, centrifuge model test results used to calibrate the analytical solution are included. In addition, comparisons of predictions with results from a series of field tests of mooring lines on various types of drag anchors are described. Comparisons include the tension in anchor, the length of mooring line on the bottom, and the angle of mooring line at the water surface buoy. Results indicate that the analytical solution method is capable of predicting the behavior of mooring lines with high degree of accuracy.

MOORING LINE ANALYSIS

The analysis of the mooring line geometric configuration is based on the limiting equilibrium method in which the detailed solutions are obtained from the static equilibrium conditions. Figure - 1 shows a schematic diagram of a mooring line element

embedded in the seafloor. T and ϕ are the axial tensile force and the inclination angle at the ends of the element. N , $(f \Delta s)$, and $(w \Delta s)$ are the normal force, the tangential force, and the buoyant weight of the mooring line element, respectively. From the static equilibrium conditions of forces along the “n” and “t” coordinates and the moment about the point “o”,

$$\begin{aligned}\Sigma F_t &= 0 \\ \Sigma F_n &= 0 \\ \Sigma M &= 0,\end{aligned}\tag{1}$$

one can solve for unknowns, N , T and ϕ . Note that previously published solutions of the embedded mooring line analysis only considered partial equilibrium conditions (7, 9, 20). The current solution method, which utilizes complete equilibrium conditions, therefore permits an additional degree of freedom in each mooring line element.

In the analysis, it is assumed that the soil tangential forces $(f \Delta s)$ remain at their limiting state at all times, since the dominant mode of the mooring line movement during deployment is sliding. The normal soil forces (N), however, remain as unknowns because of the available additional degrees of freedom and therefore can be less than those defined by the limiting state, i.e., the soil bearing capacity. It is also noted that the assumption of the mooring line element forming a circular arc as assumed in some of the previous solutions is no longer necessary in the current solution.

Eq. (1) forms the basis of recursion formulas for the detailed analysis of the embedded mooring line element in the seafloor, i.e.,

$$\begin{aligned}N &= \frac{2T_1 - f \Delta s}{\tan\phi_1 + \tan\delta} \\ T_2 &= T_1 - (f + w \sin\phi_1) \Delta s - N \tan\delta \\ \phi_2 &= \phi_1 + \frac{N - w \Delta s \cos\phi_1}{T_2}\end{aligned}\tag{2}$$

where T_1 and T_2 : axial forces at the beginning and end of the element
 ϕ_1 and ϕ_2 : mooring line inclination angle at the beginning and end of the element
 δ : interface friction angle between the mooring line and the soil
 f : tangential force per unit length
 w : buoyant weight of mooring line per unit length
 N : normal force

The solution process starts with a known mooring line inclination angle at the seafloor surface (ϕ_1). The catenary and embedded portions of the mooring line are then solved separately and added for the final solution. The following describes the solution details of the embedded portion of the mooring line.

With a known inclination angle at the seafloor surface and the horizontal force at the water surface, the mooring line axial tension at the seafloor surface (T_1) is calculated.

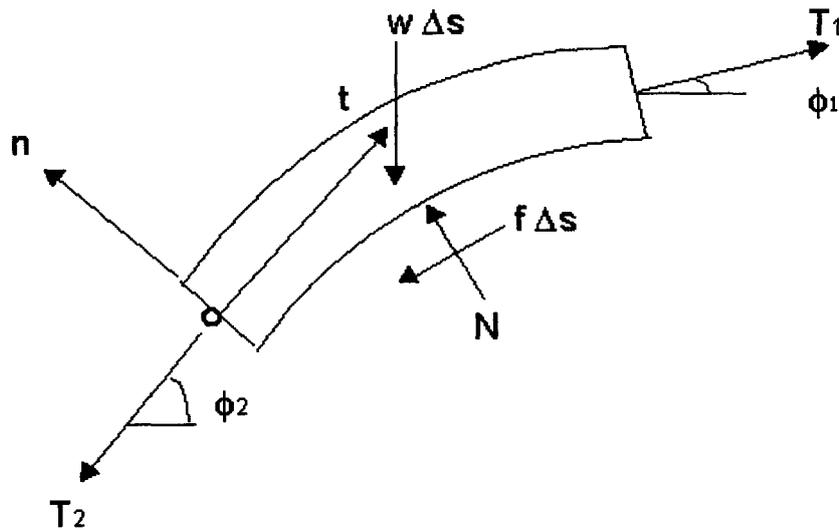


Figure – 1 Mooring Line and Free Body Diagram

Using Eq. (2), the axial tension and the inclination angle at the end of the element, T_2 and ϕ_2 , are then calculated. From the compatibility requirement, the values of axial tension and inclination angle at the end of the current element then become those at the beginning of the next element. Concurrently, the coordinates of the elements are calculated and recorded. This process continues until the depth to the element end reaches the specified anchor depth.

In the recursion equations, the element tangential force per unit length, f , is estimated assuming that the soil undrained shear strength is fully mobilized, i.e.,

$$f = EWS D \alpha \beta S_u \quad (3)$$

where EWS = equivalent diameter conversion factor for sliding force to convert mooring line diameter to circumferential area
 D = chain link or cable diameter
 α = soil adhesion conversion factor
 β = contact area conversion factor
 S_u = soil undrained shear strength.

For stud link chains, the value of EWS is obtained by converting the chain link diameter to the circumferential area of a cylinder defined by a circle encompassing two perpendicular chain links, i.e., 3.6 times π . For cables, the value of EWS is simply π .

The soil adhesion conversion factor (α) is the ratio of the adhesion between the mooring line and the soil vs. the soil cohesion. The contact area conversion factor (β) is the ratio of the true contact area between the mooring line and the soil versus the surface area of a cylinder defined by the mooring line. In case of chain, the cylinder is defined by a circle encompassing two perpendicular chain links. For cable, the cylinder is simply

defined by the cable diameter. The value of β may be less than 1.0, if a separation occurs on the backside of the mooring line while it is deployed.

The value of the normal force, N , is limited to be no greater than the soil bearing capacity, i.e.,

$$\begin{aligned} N &< N_{\max} = q \Delta s \\ q &= \text{EWB } D S_u N_c \end{aligned} \quad (4)$$

where q = bearing capacity of soil per unit length

EWB = equivalent diameter conversion factor for normal force to
convert mooring line diameter to projected bearing area

N_c = soil bearing capacity factor.

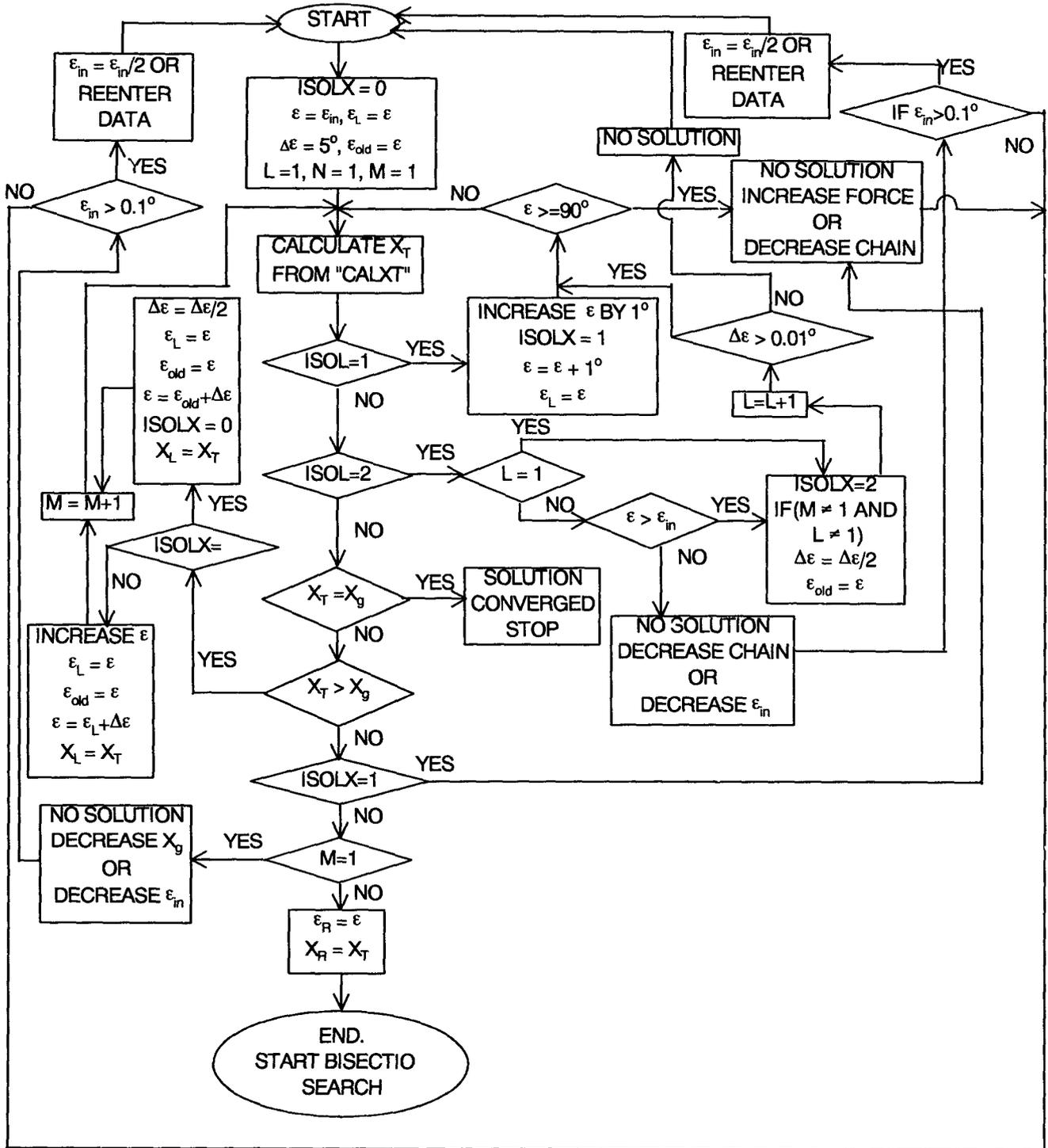
For stud link chains, the value of EWB is obtained by converting the chain link diameter to the diametric projectional area of a cylinder defined by a circle encompassing two perpendicular chain links, i.e., 3.6. For cables, the value of EWB is 1.0.

When the horizontal distance between the anchor and buoy or the total length of the mooring line between the anchor and buoy is specified, a portion of the mooring line may lie on the seafloor surface if the calculated total length of the mooring line with zero mooring line inclination angle at the seafloor surface is less than the specified total length of the mooring line. In such a case, the solution requires an additional step for the determination of the length of the mooring line lying on the seafloor surface. This requires satisfaction of the following two conditions; (1) the mooring line inclination angle at the seafloor surface remains zero, and (2) the mooring line tension at the beginning of the embedded portion is the horizontal tension at the water surface minus the sum of soil tangential force that develops underneath the mooring line lying on the seafloor surface. Since the length of the mooring line lying on the seafloor surface is an unknown, it is determined iteratively by initially assuming that length and comparing the resulting total mooring line length with the specified total length.

Figure – 2 shows the flow chart describing the solution steps for the determination whether a portion of the mooring line lies on the seafloor surface.

Chain-Soil Analysis Program

A computer software, Chain-Soil Analysis Program (CSAP), has been developed to perform the design and analysis of single-leg chain/cable mooring lines associated with drag/fixed anchors embedded in a cohesive or cohesionless seafloor. The software can determine the geometric configuration of and developed tensions within the mooring line at deployment. It can incorporate (1) any combination of mooring line segments such as the chain, cable, or synthetic wire, (2) sinkers attached to mooring lines, and (3) layered seafloor soil conditions or depth-dependent seafloor soil properties. It also includes the calculation of the $P - \Delta$ relationship, i.e., the relationship between the applied horizontal load at the buoy not exceeding the deployment load and the resulting horizontal movement of the buoy. The analysis allows three solution criteria, namely, the horizontal distance between the anchor and buoy, the total length of the mooring line between the anchor and buoy, or the mooring line exit angle at the seafloor surface. It is based on the assumption that all materials behave completely elastically.



CASE OF A PORTION OF MOORING LINE LYING ON THE SEAFLOOR SURFACE

Figure – 2 Determination of Whether a Portion of Mooring Line Lying on the Seafloor Surface

Major input data for CSAP are the values of the horizontal tension at the buoy, water depth, and depth to the anchor from seafloor, in addition to the material and geometric parameters. The program is capable of analyzing mooring lines embedded in either cohesive or cohesionless soils, or soils having both cohesion and friction.

When a mismatch occurs among the inputted parameters, the program stops the computation and asks the user to reenter a new set of input parameters. Several possible reasons for a mismatch include: (1) the mooring line size is too large or too small for given force at the buoy, (2) the anchor is located too deep, (3) the specified total length of the mooring line or the distance between the anchor and the buoy are too long or too short, or (4) the initial angle of mooring line to the horizontal at the seafloor surface is too high.

The detailed solution of a multi-segmented mooring line embedded in a layered seafloor soil is obtained from an iterative search. The initial material and geometric parameters to be used in the analysis are obtained from the assumed length of the buried mooring line. The results of the analysis with these assumed parameters are then compared with the true material properties of the multi-segmented mooring line, which in turn determines the necessity of additional iterations. For instance, at the first iteration, by comparing the solution of the buried length of the mooring line with the specified length of the first segment of the mooring line attached to the anchor, one can determine whether the entire first segment is completely buried or not. If it is determined that only part of the first segment of the mooring line is buried within the seafloor, complete solutions of the buried portion and the catenary portion of the mooring line are obtained from an additional iterative search. On the other hand, if it is determined that the entire first segment of the mooring line is buried, the buried portion of the mooring line is analyzed assuming that the remaining portion of the buried length of the mooring line beyond the first segment consists of second segment mooring line. Similar analysis, as described above, will reveal whether the entire second segment of the mooring line is buried within the seafloor or not, which in turn determines the necessity of further iterations. This process continues until the complete details of the mooring line composition within the seafloor are identified, which is followed by the analysis of the catenary portion of the mooring line. The iteration stops when the relative error between two consecutive solutions of the specified criterion – the total length of the mooring line or the horizontal distance between the anchor and buoy – is less than the value specified.

The analytical solution can also calculate the load vs. deflection ($P - \delta$) relationship at the buoy at the end of the mooring line analysis. A relationship between the various magnitudes of loads at the buoy and the corresponding horizontal displacements of the buoy are calculated. Figure - 3 shows the flow chart describing the steps involved in the $P - \delta$ curve calculation.

Stretch of Mooring Line due to Applied Force at Buoy

Mooring lines have certain axial stiffness and, therefore, will be stretched upon tensioning. The seafloor soil will also experience deflection caused by the compression developed at the underside of the mooring line due to its elasticity.

Typical mooring lines consist of either chain or cable. It is therefore reasonable to assume that the bending and shear resistances are negligible. The majority of the

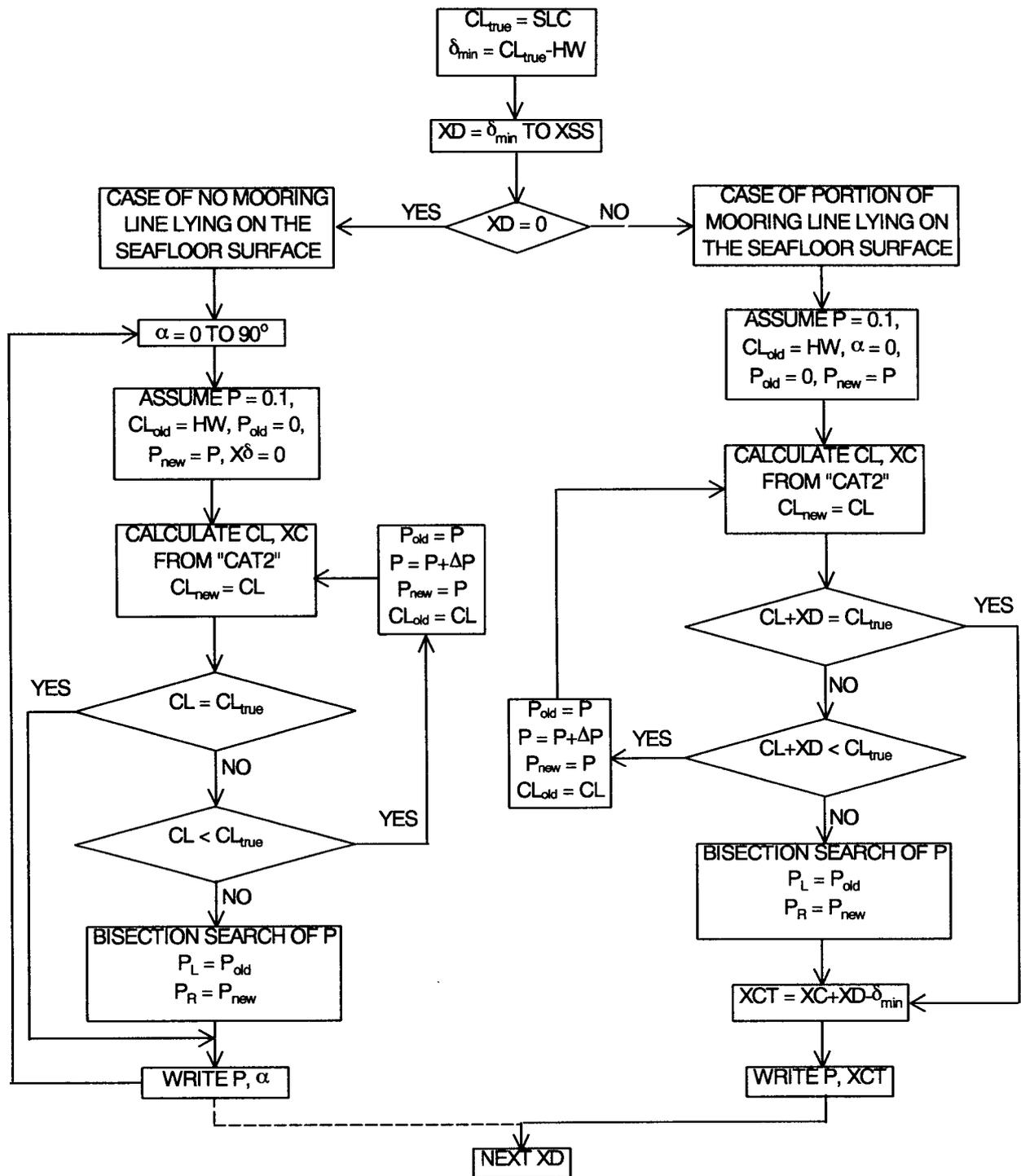


Figure - 3 P - δ Calculation

mooring line stretch upon tensioning will result from the axial stiffness of the mooring line.

Mooring lines after deployment may consist of three segments, i.e., the portion buried in seafloor, the portion lying on the seafloor surface, and the portion suspended in the water. When a mooring line is tensioned, the analytical solution method calculates the developed tension force within each element within these segments, starting from the anchor to the surface buoy. Since it is assumed that only the axial stiffness contributes to the stretch of the mooring line, the elastic stretch of individual mooring line element can be calculated from

$$\delta_i = \frac{F_i l_i}{(EA)_i} \quad (5)$$

where δ_i = axial stretch of element i
 F_i = axial tension of element i
 l_i = length of element i
 $(EA)_i$ = axial stiffness of element i

The total stretch of the entire mooring line due to its axial stiffness can then be obtained by summing the stretches of all mooring line elements.

$$\delta = \sum_{i=1}^n \delta_i \quad (6)$$

where δ = total stretch of entire mooring line
 n = number of mooring line elements

In addition to the axial stiffness of the mooring line, the seafloor soil elasticity will also contribute to the change in geometry of the mooring line as schematically explained in Figure – 4.

It is assumed in this study that the behavior of the seafloor soil upon normal force application is completely described with the elastic foundation theory (21), i.e., the normal deflection of the soil is directly proportional to the applied normal load as shown below.

$$p = k y_n \quad (7)$$

where p = normal pressure
 k = subgrade reaction coefficient
 y_n = normal deflection.

The soil subgrade reaction coefficient can be obtained from literature (8, 11, 18, 19).

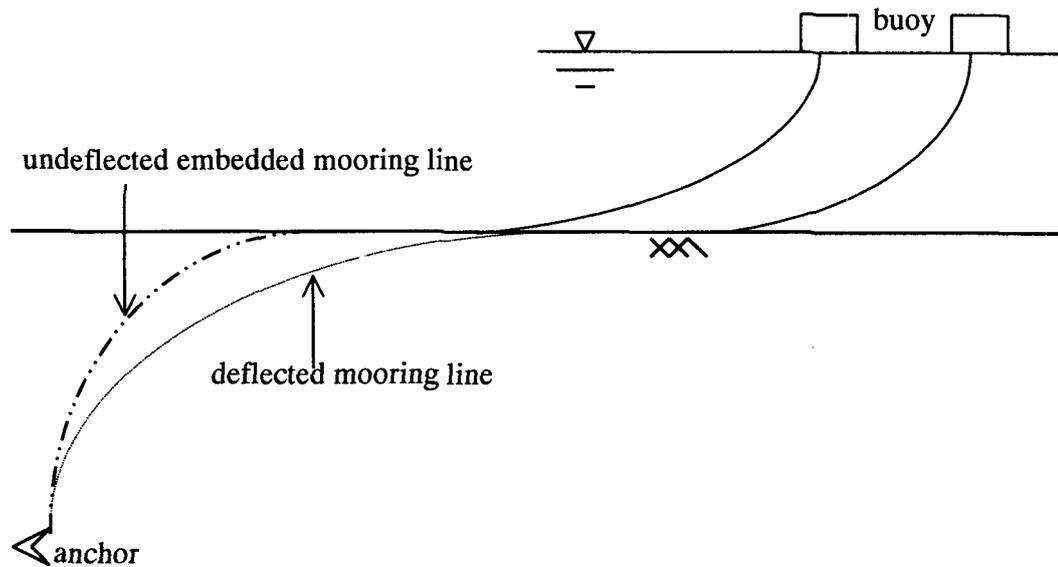


Figure – 4 Schematic Diagram of Mooring Line Deflection

CENTRIFUGE MODEL TESTS

Model mooring lines were tested to verify the analytical solution under an elevated acceleration field within the centrifuge to closely simulate the nonlinear stress-dependent behavior of the soil (10). A centrifuge, located at the University of Colorado, Boulder, was used for this purpose. It has a capacity of 440 g-tons with a capability of accelerating 2.2 ton payload to a maximum acceleration of 200 g's. It has a radius of 18 ft. from the centrifuge center to the top of the model bucket. The model bucket can be as large as 4 ft. x 4 ft. x 3 ft.

Experiments were conducted by pulling a mooring line at its end with a pulling mechanism while the other end of the mooring line was anchored at a fixed point. Both ends of the line were equipped with load cells. The final mooring configuration was established from the post-test dissection of the soil mass.

The clay used was Speswhite fine china kaolin mixed to an initial water content of 137 % which corresponded to a void ratio of $e = 3.64$. The sample was allowed to consolidate for 15 hours at 80 g's before the first vane test was performed. The undrained shear strengths (S_u) of the soil were measured in-flight after the consolidation by a miniature vane and correlated with additional data derived from the void ratio vs. shear strength relationship of the test clay. The results indicated that the soil undrained shear strength remained constant at approximately 65 psf from the surface to a depth of 1.5 in. and then increased at a rate of 43 psf/in., indicating higher degrees of overconsolidation near the surface. This corresponds to S_u of 65 psf from zero to 10 ft. and 6.5 psf/ft. below 10 ft. in prototype.

Table – 1 shows the test matrix of the first tub. Preparation for each test required the following steps; (1) moving the take-up spool, (2) switching of entire linear variable

Test	Type of Mooring	Anchor Depth (in.)	Max. Static Load (lbs)
1 - 1	Ball Chain	2	50
1 - 2	Ball Chain	4	50
1 - 3	Ball Chain	6	50
1 - 4	Aircraft Cable	6	50

Table – 1 Mooring Lines for Centrifuge Tests

distance transducer (LVDT) measurement system to a new track, and (3) resetting the mooring line configuration. This required stopping the centrifuge for about one to two hours during which time the sample swelled, and thus reconsolidation was needed before the pulling test.

Model chains were fixed at depths of 2 in., 4 in., and 6 in. They were tested under a centrifugal acceleration equal to 80 times the gravitational acceleration. The model chain utilized a ball chain having a ball diameter of 3/16 in. and was loaded to 46.88 lbs horizontally at the seafloor surface. Note that the corresponding prototype geometric dimensions become model dimensions multiplied by the applied centrifugal acceleration level as a multiple of the gravitational acceleration. However, the corresponding prototype load is obtained by multiplying a square of the applied acceleration level, e.g., the prototype applied load is equivalent to 300 kilo-pounds (kips) under 80 g acceleration.

Results

Results indicate that the mooring cable geometry (as influenced by the chasing wires which were used to locate the geometry of mooring lines) can be estimated very accurately using the values of the cable bearing capacity factor $N_{cw} = 7 \sim 9$ and the cable sliding adhesion factor $\alpha_w = 0.5 \sim 3.2$. However, the measured mooring cable force at the fixed end is significantly influenced by the values of N_{cw} and α_w . The measured mooring cable force at the fixed end could be obtained if the value N_{cw} of 9 is used.

For mooring chains, results indicate that the trajectory is primarily influenced by the value of chain bearing capacity factor N_{cc} , whereas the force at the fixed end is primarily influenced by the value of the chain sliding adhesion factor α_c . The mooring chain geometry (as influenced by the chasing wires) can be estimated with reasonable accuracy using the value of $N_{cc} = 14$. Although the difference in value of N_{cc} is noted with and without considering the effect of chasing wires, the difference is not significant.

From the results of the centrifuge study described, the optimum values of the N_{cc} and α_c have been determined as follows.

For mooring cable, $N_{cw} = 9$

$\alpha_w = 1.4$

For mooring chain, $N_{cc} = 14$

$\alpha_c = 1.4$

COMPARISON WITH FIELD TESTS

A series of field tests on drag embedment anchors were performed by the Naval Facilities Engineering Service Center in Indian Island in Puget Sound, Washington (12, 13).

The Indian island seafloor consisted of normally consolidated soft silty clay with shell fragments and was classified as an organic silty clay of high plasticity. The particle size was almost evenly distributed between silt and clay. The liquid limit and water content values were relatively high and approximately equal, varying little with depth up to 28 feet. Values ranged from 110 to 160 for the water content and 117 to 142 for the liquid limit. The shear strength increased almost nearly from zero at the surface to 216 psf at 21 feet.

Figures - 4 and 5 show the schematics of the test setup. The mooring line was pulled by the barge, dragging the anchor under the seafloor with the total mooring line length remaining the same all the time. Instruments on the anchor, the mooring line, and the barge recorded the movements and tensions of the anchor and mooring line.

The details of the anchors and mooring lines used for the tests are listed in Table - 2. It describes the anchor type, the anchor weight and the mooring line details. Please refer the references (14, 15, 16, 17) for the detailed performance of various anchors.

Comparison

Major input data for the analytical comparison with field test results are the values of the horizontal tension at the buoy, water depth, depth to anchor from seafloor, and friction factor at the seafloor surface, in addition to the material and geometric parameters.

The seafloor soil strength was described by a linearly increasing rate with depth of about 10 psf/ft, starting from zero strength at the surface. The friction factor describes the mooring line - soil interaction behavior at the seafloor surface.

The measured results from the field tests included the anchor force, the mooring line inclination angle at the buoy, and the length of the mooring line on the bottom. The length of the mooring line on the bottom is the total length of the mooring line buried in the seafloor and lying on the seafloor surface. These were compared against the results from analytical solutions.

In the analytical solution, the tangential force developed along the mooring line segment buried within the seafloor is described based on the conventional Mohr - Coulomb shear strength theory, i.e.,

$$F = c l + N \tan \delta \quad (8)$$

where F = tangential force

c = soil cohesion

l = mooring line segment length

N = normal force

$\tan \delta$ = interface friction coefficient between the mooring line and the soil

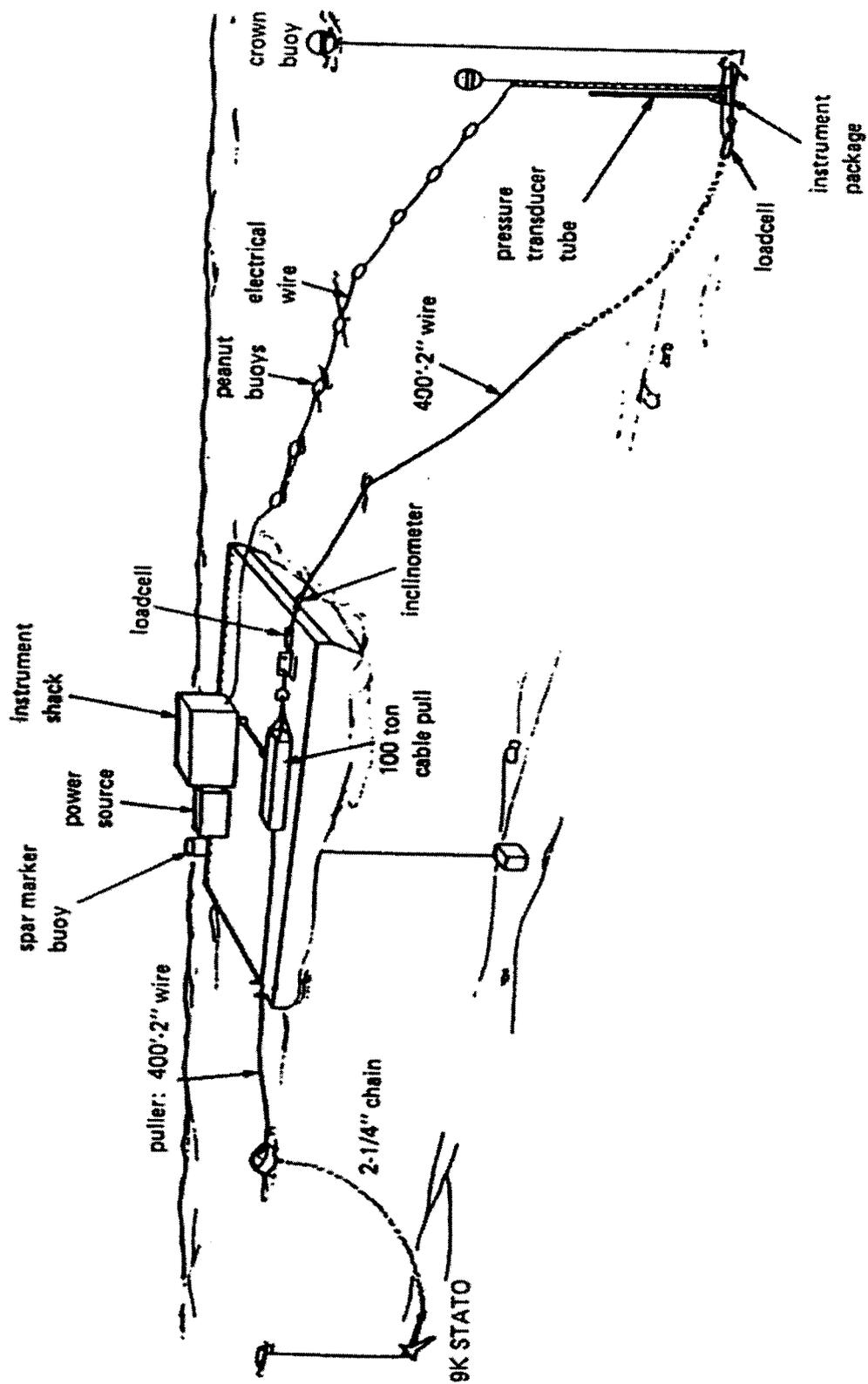


Figure - 4 Anchor Test Setup

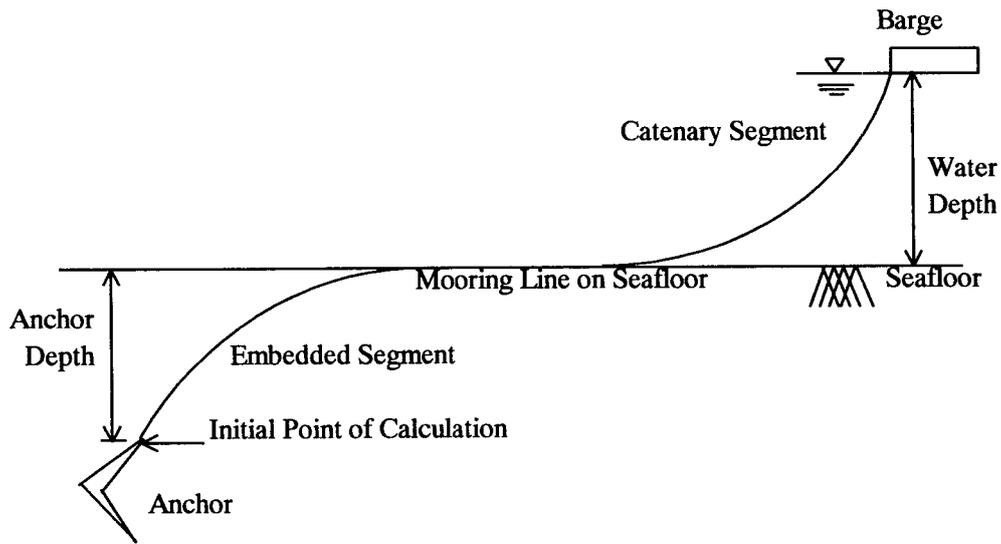


Figure - 5 Anchor - Mooring Line System

The interface friction coefficient, $\tan\delta$, is typically expressed as a fraction of the soil internal friction coefficient, $\tan\phi$. This description of the tangential force has been found to be very representative for mooring line segments buried within the seafloor. However, the tangential force developed between the mooring line and the soil at the seafloor surface needs a special attention, particularly for saturated cohesive soils which follow the $\phi = 0$ behavior. Therefore, the surface friction factor between the mooring line and the soil is introduced to describe the tangential force developed along the mooring line lying on the seafloor surface, i.e.,

$$F = c l + N \Delta \quad (9)$$

where Δ = surface friction factor.

The magnitude of the surface friction factor can be evaluated from the field test results as explained below.

At the beginning of the test, the entire mooring line either lies on the seafloor surface or is suspended in the water. When the mooring line is tensioned, the sum of the force at the anchor and the friction force along the mooring line must equal to the horizontal tension applied at the deck (Figure - 6). Since the soil cohesion at zero depth is negligible, the surface friction factor, Δ , can be calculated from Eq. (9), i.e.,

$$\Delta = \frac{F}{N} \quad (10)$$

Test No.	Seafloor type	Anchor type	Anchor weight (lbs)	Mooring line description
170-1	Silt	Stato	1070	90 ft. 2 in. C; 360 ft. 2.5 in. C; 400 ft. 1-5/8 in. W; 346 ft. 2 in. W
172-7	Silt	Stockless	11370	90 ft. 2 in. C; 360 ft. 2.5 in. C; 400 ft. 1-5/8 in. W; 346 ft. 2 in. W
172-8	Silt	Stockless	11370	90 ft. 2 in. C; 360 ft. 2.5 in. C; 400 ft. 1-5/8 in. W; 346 ft. 2 in. W
172-9	Silt	Stockless	5950	90 ft. 2 in. C; 360 ft. 2.5 in. C; 400 ft. 1-5/8 in. W; 346 ft. 2 in. W
172-10	Silt	Stockless	5950	90 ft. 2 in. C; 360 ft. 2.5 in. C; 400 ft. 1-5/8 in. W; 346 ft. 2 in. W
174-13	Silt	Stockless	5950	135 ft. 2 in. C; 360 ft. 2.5 in. C; 400 ft. 1-5/8 in. W; 346 ft. 2 in. W
174-14	Silt	Stockless	5950	135 ft. 2 in. C; 360 ft. 2.5 in. C; 400 ft. 1-5/8 in. W; 346 ft. 2 in. W
176-23	Silt	Stato	3500	135 ft. 2 in. C; 360 ft. 2.5 in. C; 400 ft. 1-5/8 in. W; 346 ft. 2 in. W
176-25	Silt	Stato	6600	135 ft. 2 in. C; 360 ft. 2.5 in. C; 400 ft. 1-5/8 in. W; 346 ft. 2 in. W
208-5	Silty Clay	Two fluke	9800	180 ft. 2.0 in. C; 270 ft. 3 in. C
209-12	Silty Clay	Stevfix	11000	90 ft. 3.0 in. C; 180 ft. 2.0 in. C; 270 ft. 3 in. C

Note : C = Chain, W = Wire

Table - 2 Description of Anchors and Mooring Lines of Indian Island Tests

where F = barge horizontal tension minus measured anchor force at zero penetration
 N = total weight of mooring line on seafloor surface at zero penetration.

Using the field measurements at the very beginning of the tests, the surface friction factors at the seafloor surface were obtained as shown in Table - 3.

As described in the previous chapter, the centrifuge test results yielded the values of the chain bearing capacity factor (N_{cc}), the cable bearing capacity factor (N_{cw}), the chain sliding adhesion factor (α_c), and the cable sliding adhesion factor (α_w) associated with the clay. These values obtained from the centrifuge tests were used for the verification of the analytical solution with field test results. Table - 4 indicates the details of these factors together with the diameter conversion factors used in the verification with field test results.

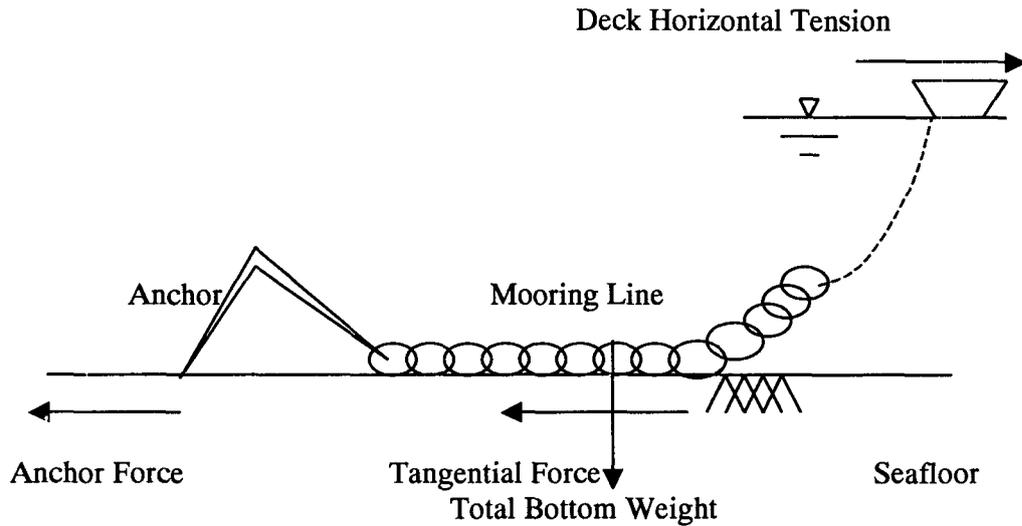


Figure – 6 Anchor and Mooring Line on Seafloor

Test Number	Anchor Crown Depth (ft)	Water Depth (ft)	Deck Horizontal Force (lbs)	Anchor Force (lbs)	Deck Horiz. Force - Anc. Force (lbs)	Total Bottom Weight (lbs)	Surface Friction Factor
170-1	89.7	86.4	13400	2800	10600	21843.9	0.485
172-7	80.6	78.8	17300	2500	14800	20937	0.707
172-8	91.2	90.8	20300	3300	17000	20646.2	0.823
172-9	93.2	92.2	17500	200	17300	25801.9	0.670
172-10	92	92	23100	800	22300	25004.7	0.892
174-13	87.2	86.9	19600	No data	***	27198.4	***
174-14	89.2	88.9	22200	No data	***	26894.7	***
176-23	80.8	81.9	28700	600	28100	22979.8	1.223
176-25	93	89.3	41700	No data	***	23461.4	***
208-5	88	89	13800	7600	6200	20250.7	0.306
209-12	85.8	88	13200	100	13100	28303.1	0.463

Table – 3 Surface Friction Factors of Indian Island Tests

The mooring line consists of three typical segments, as shown in Figure - 5; the embedded segment, i.e., the portion of mooring line completely buried within the seafloor; the mooring line segment lying on the surface of the seafloor; and the catenary segment, i.e., the mooring line suspended in the water (6).

Item	Value (dimensionless)
Diameter Factor for Chain Bearing (EWBc)	0.3
Diameter Factor for Cable Bearing (EWBw)	0.0833
Diameter Factor for Chain Sliding (EWS _c)	0.94
Diameter Factor for Cable Sliding (EWS _w)	0.2618
Chain Bearing Capacity Factor (N_{cc})	14
Cable Bearing Capacity Factor (N_{cw})	9
Chain Slide Adhesion Factor (α_c)	1.4
Cable Slide Adhesion Factor (α_w)	1.4

Table - 4 Constant Input Data of Indian Island Tests

The results of field tests, except whose surface friction factors could not be determined due to insufficient field data, on the axial force at anchor, the mooring line inclination angle at buoy, and the mooring line length on bottom have been compared with the analytical predictions.

Figures - 7 through 9 show the summary of comparisons between the measured and the predicted values. As can be seen from Figure - 7, the measured anchor forces agree very well with the analytical solutions. The mooring line inclination angles at buoy also show very good agreement between the measured and the calculated values, as shown in Figure - 8, for all tests. Figure - 9 indicates that the predicted values of the mooring line on the bottom slightly overestimate the measured values. The discrepancy between the measured and the predicted values may be in part due to the variation in soil conditions at the test site. Additional study needs to be conducted in characterizing the load transfer mechanism at the seafloor surface to improve the accuracy of the analytical solution.

CONCLUSIONS

An analytical solution that can calculate the key responses of mooring lines upon tensioning is described. The effectiveness of the solution was validated through comparisons with the field mooring line tests conducted in cohesive seafloor. Comparisons include the anchor force, the mooring line angle at the buoy, and the mooring line length on the bottom. Although slight deviation exists between the measured and the predicted values, results indicate that the developed analytical solution is capable of predicting the essential responses of mooring lines with high degree of accuracy. This discrepancy may be in part due to the variation in soil conditions at the test site.

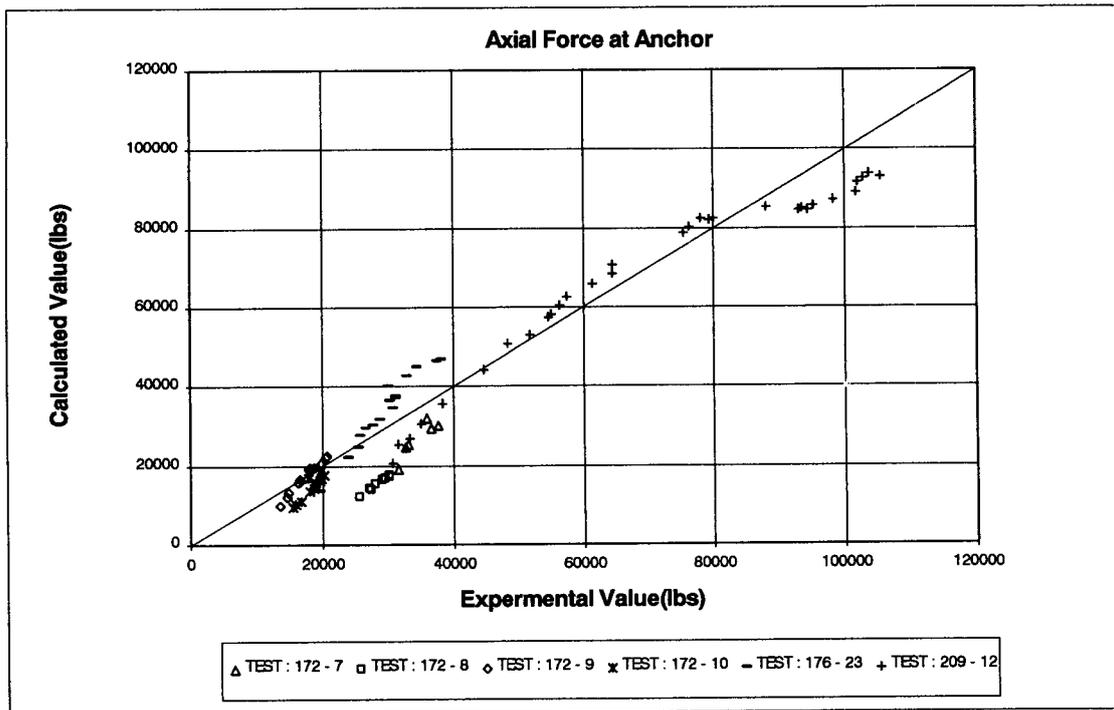


Figure – 7 Comparison of Axial Force at Anchor

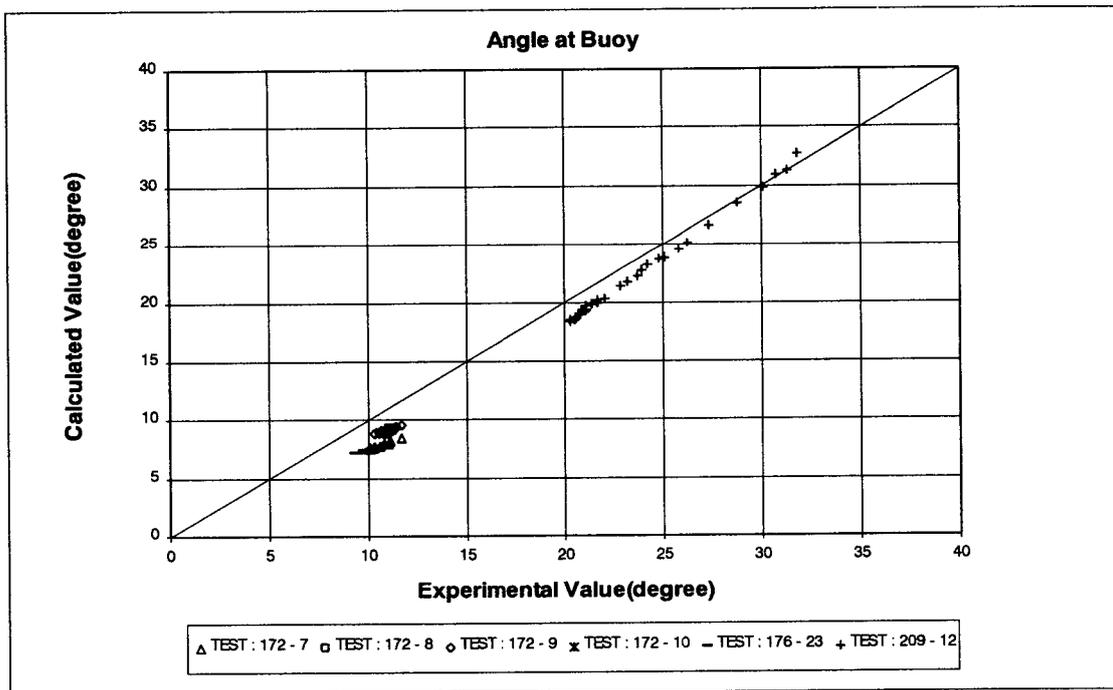


Figure – 8 Comparison of Angle at Buoy

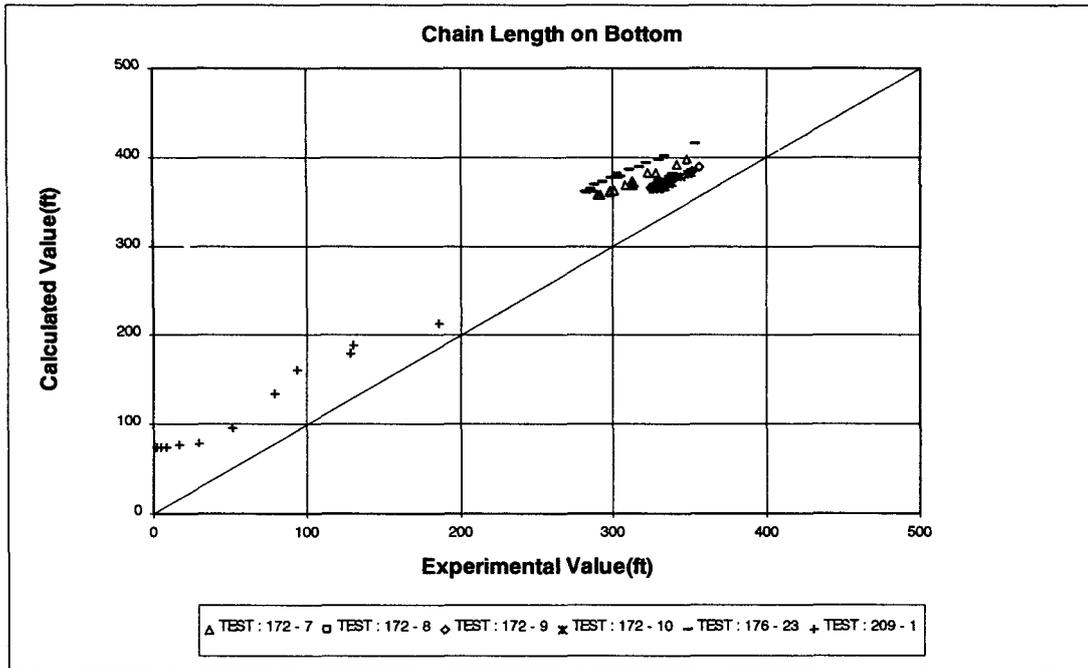


Figure – 9 Comparison of Chain Length on Bottom

The validation of the analytical solution is limited to cohesive seafloor soils as described in this paper. For the analytical solution to be completely validated, it is absolutely essential to expand the validation process with either field or centrifuge test results in sandy seafloor soils.

It is noted that the analytical solution and its validation are limited to static behavior. Similar verification work is needed for a dynamic analysis of mooring lines.

ACKNOWLEDGMENTS

The material presented in this paper is based on the author's previous work and the Ph.D. dissertation by Heuisoo Han. The author is grateful to the technical and financial supports provided by the U.S. office of Naval Research and the Naval Facilities Engineering Service Center.

REFERENCES

1. Bang, S., "Anchor Mooring Line Computer Program User Manual," Contract Report CR - 6020 - OCN, Naval Facilities Engineering Service Center, June, 1996.

2. Bang, S., "Anchor Mooring Line Computer Program User Manual, Version 2," Naval Facilities Engineering Service Center, 1998.
3. Bang, S., "Use of Suction Piles for Mooring of Mobile Offshore Bases," Quarterly Progress Report to the Office of Naval Research, Sep., 1999.
4. Bang, S., Han, H., and Taylor, R. J., "Calibration of Centrifuge Model Tests on Mooring Lines," *9th Offshore and Polar Engineering Conference*, 1999.
5. Bang, S., Taylor, R. J., Jie, Y., and Kim, H., "Analysis of Anchor Mooring Line in Cohesive Seafloor," Transportation Research Record, No. 1526, 1996.
6. Brian Watt Associates, Inc., "Development of Methodology to Predict Anchor Performance in Marine sediments, Phase 2," Technical Report, Naval Facilities Engineering Service Center, June 1981.
7. Brian Watt Associates, Inc., "A Method for Predicting Drag Anchor Holding Capacity," Report No. CR 83.036, 1983.
8. Das, B. M., *Principles of Foundation Engineering*, 3rd Ed., PWS Publishing Co., 1995.
9. Degenkamp, G. and A. Dutta., "Soil Resistance to Embedded Anchor Chain in Soft Clay," *Journal of Geotechnical Engineering*, Vol. 115, No. 19, 1989.
10. Law, H. K., et. al., "Centrifuge Testing for Dynamic Anchor Line Modeling," A Report submitted to Naval Facilities Engineering Service Center, Univ. of Colorado, Boulder, Oct., 1994.
11. Scott, R. F., *Foundation Analysis*, Prentice-Hall, 1981.
12. Taylor, R. J., "Conventional Anchor Test Results at San Diego and Indian Island," Technical Note No. N - 1581, Naval Facilities Engineering Service Center, July 1980.
13. Taylor, R. J., "Drag Embedded Anchor Tests in Sand and Mud," TN No. N- 1635, Naval Facilities Engineering Service Center, 1982.
14. Taylor, R. J., "Single and Tandem Anchor Performance of the New Navy Mooring Anchor: The NAVMOOR Anchor," Technical Note No. N - 1774, Naval Facilities Engineering Service Center, July 1987.
15. Taylor, R. J., and Chern, C., "Multiple STOCKLESS Anchors for Navy Fleet Moorings," Technical Sheet No. 83-05, Naval Facilities Engineering Service Center, February 1983.
16. Taylor, R. J., and Chern, C., "The NAVMOOR Anchor," Technical Sheet No. 87-05, Naval Facilities Engineering Service Center, May 1987.
17. Taylor, R. J., and Walker G. R., "Model and Small- Scale Tests to Evaluate the Performance of Drag Anchors in Combination," Technical Note No. N - 1707, Naval Facilities Engineering Service Center, October 1984.
18. Terzaghi, K., "Evaluation of Coefficient of Subgrade Reaction," *Geotechnique*, Vol. 4, 297, London, 1955.
19. Vesic, A. S., "Bending of Beams Resting on Isotropic Solid," *Journal of the Engineering Mechanics Division, ASCE*, Vol.87, EM 2, 1961.
20. Vivatrat, V., P. J. Valent, and A. A. Ponterio., "The Influence of Chain Friction on Anchor Pile design," *Proc., 14th Annual Offshore Technology Conference*, Paper No. 4178, 1982.
21. Winkler, E., *Die Lehre von Elastizität und Festigkeit*, Prague, 1987.